Elephant DOA Estimation using a Geophone Network

Gustav Zetterqvist, Erik Wahledow, Philip Sjövik, Fredrik Gustafsson and Gustaf Hendeby

Elephant DOA Estimation using a Geophone Network

Gustav Zetterqvist, Erik Wahledow, Philip Sjövik, Fredrik Gustafsson, Gustaf Hendeby
Division of Automatic Control, Linköping University, SE-581 83 Linköping, Sweden
Email: gustav.zetterqvist@liu.se, {eriwa458, phisj589}@student.liu.se,
{fredrik.gustafsson, gustaf.hendeby}@liu.se

***Abstract*—Human-wildlife conflicts are a global problem which is central to the Global Goal 15 (life on land). One particular case is elephants, that can cause harm to both people, property and crops. An early warning system that can detect and warn people in time would allow effective mitigation measures. The proposed method is based on a small local network of geophones that sense the seismic waves of elephant footsteps. It is known that elephant footsteps induce low frequency ground waves that can be picked up by geophones in the ground. First, a method is described that detect the particular signature of such footsteps, and then the detections are used to estimate the *direction of arrival* (DOA). Finally, a Kalman filter is applied to the measurements in order to track the elephant. Field tests performed at a local zoo shows promising results with accurate DOA estimates at 15 meters distance and acceptable accuracy at 40 meters.**

***Index Terms*—Elephants, Detection, Direction of Arrival, Kalman filter, Geophone network**

I. Introduction

One of the main problems connected to national parks is human-wildlife conflicts. In 2020, over 90 people were killed by wildlife in Kenya, and six people died by elephants in Amboseli National Park alone [1]. Hundreds of casualties caused by elephants are reported in India each year and local communities suffer from destroyed fields and property [2]. It is costly to protect properties such as schools using fence lines and even then it often fails due to lack of maintenance [3]. Thus, an automated warning system capable of detecting and localizing elephants long before they arrive could prove to be very useful. Here, the seismic waves from elephants' footsteps are used to detect and locate the elephants. Mitigation measures may include lights, sounds and smells disliked by the elephants, or even release of bee swarms.

Detection of seismic events using geophones is a well studied topic. Studied seismic events include human footsteps [4], [5], vehicles [6], [7], landslides [8], etc. Detecting elephants using geophones has also been carried out in the past. The general idea is to utilize that the pressure waves generated by elephants can travel very far [9]–[11]. However, in most cases it is not the footsteps that are detected, but rather vocalization, also known as rumbles, that generates seismic components [10], [11]. Rumbles are produced by the elephants for various reasons, e.g., to warn about a threat, as a greeting or to advertise mating to the other sex [12]. The detection of elephant footsteps has previously been studied, e.g., [13] use a frequency analysis approach and [14] use a machine learning approach. However, the level of detail in the description make these methods difficult to replicate.

The seismic waves produced by elephant vocalization have additionally been used for localization of elephants [11]. When it comes to safeguarding a village, it is essential to localize the elephants as they are moving. Therefore, the approach here is to use their footsteps for localization. Tracking a seismic source by using a network of geophones has been done before in a seismic security system [15]. However, the application to elephants is novel.

This paper presents a well-documented approach for the tracking of elephant footsteps using seismic signatures. Our methodology incorporates a frequency-based approach to detect the signature of elephant footsteps. Thereafter, the *direction of arrival* (DOA) of the detected footstep is accurately estimated using a sensor fusion approach. Finally, the movement of elephants is effectively tracked using a Kalman filter and a gating technique that rejects unlikely DOA estimates. Our results demonstrate the effectiveness of this approach, validated at distances ranging from 15 to 40 meters, which is promising for practical application in the field.

The paper is outlined as follows. The signal model and characteristics are presented in Section II, along with the proposed classification and DOA estimation methods. Field trials and the experimental setup are outlined in Section III, while Section IV describes the seismic signal of an elephant footstep, the properties of the ambient noise as well as the overall results. Finally, the conclusions are presented in Section V.

II. Signal processing chain

In this section the signal model and characteristics are presented as well as the methods for detection, DOA estimation and tracking.

A. Signal Model

It is assumed that geophone i measures the signal

$$y_i(t) = \sum_n s\left(t - \delta_n + \tau_i\left(\phi(t)\right)\right) + e_i(t), \tag{1}$$

where

G. Zetterqvist has received funding from ELLIIT. This work was partially funded by the Wallenberg AI, Autonomous Systems and Software Program (WASP) funded by the Knut and Alice Wallenberg Foundation.

- $s(t)$ is the seismic signature of an elephant footstep at time $t = 0$.
- δ_n denotes the time for footstep number n.
- $\phi(t)$ is the DOA at time t. The array is assumed to satisfy a far-field assumption, i.e., the DOA is the same for all geophones.
- $\tau_i(\phi)$ is the geometric delay to geophone i with respect to the local origin of the array (where $\tau(\phi) = 0$ for all ϕ).
- $e_i(t)$ is all non-interesting signals measured by geophone i, e.g, electrical noise, sensor bias or other ambient signals.

B. Signal characteristics

Seismologic sources produce both body and surface waves. The surface waves tend to have a low frequency, usually not higher than 200 Hz, and spread in a two-dimensional space which results in a decay of $1/\sqrt{r}$. On the other hand, body waves spread in a three-dimensional space, resulting in a decay of $1/r$, where r is the traveled distance of the wave. There are two types of surface waves, Rayleigh and Love waves. Rayleigh waves cause an elliptical motion in the vertical plane while Love waves cause horizontal ground movement. Rayleigh waves tend to be stronger from near-surface seismic sources as opposed to deeper underground sources. Furthermore, Rayleigh waves tend to be stronger than other wave forms on the Earth's surface, hence most of the shaking felt from earthquakes originates from Rayleigh waves [16].

Measurements of elephant rumbles and "foot stomps" were conducted by O'Connell-Rodwell et. al. [10] using both microphones and geophones. The findings indicate that a "foot stomp" has a duration of 103–250 ms, a mean frequency of 20.04 Hz, and a wave propagation speed of 248–264 m/s. The slow propagation speed suggests that it is a Rayleigh wave [10].

An important aspect of the seismic signals are the noise sources. Every location has different noise characteristics, but the most common noise sources around 0.5–50 Hz are wind, thunder and cultural noise. Winds usually creates seismic waves close to the surface at around 0.5–5 Hz [17], while the spectra of thunder is broadband around 5–100 Hz with a peak around 6–13 Hz [18]. Cultural noise is a term associated with man or man-made machines, e.g., power plants, factories, trains, highways, etc. Power plants have a narrowband seismic signal around 50 or 60 Hz with harmonics and subharmonics dependent on the environment [17]. The seismic footprint of trains and cars is broadband with a peak around 15 Hz [19].

C. Pre-filtering and detection

To analyze if there are elephants present, and if so where, the signal is split into segments with overlapping samples. Since the purpose is to run the system in real time, it is not possible to run the algorithm for each new sample as the computational load would be too heavy. If an elephant footstep have a duration of $N/2$ samples, using a segment that is N samples long and has $N/2$ overlapping samples with adjacent segments, the full footstep is guaranteed to be present in at least one segment.

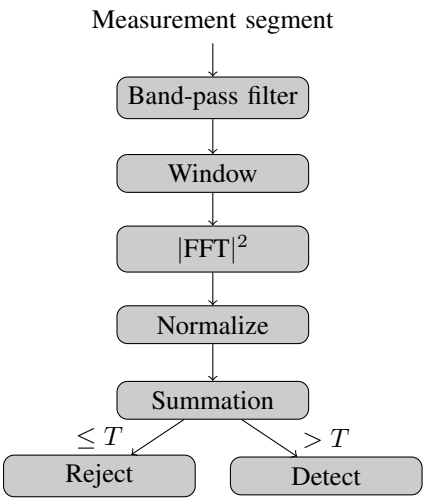

Fig. 1: An overview of the detection algorithm.

The method for detection of an elephant footstep in the signal segment is based on the frequency content of the signal. First, the signal segment is filtered with a band-pass filter to remove sensor bias, high-frequency noise and other ambient signals while preserving the elephant footstep. This filter is run both forwards and backwards in time to avoid phase shifting. As the Fourier transform assumes that the length of the signal is infinite, the signal is then windowed using a Hanning window to prevent leakage.

Subsequently, the *Fast Fourier Transform* (FFT) is computed whereupon the magnitude of the FFT (the periodogram) is computed. To make the algorithm independent of the strength of the signal, the periodogram is normalized with the total energy of the periodogram. Summing the energy of the normalized periodogram around the main frequencies of an elephant footstep thus provides an estimate of how strongly the signal resembles an elephant's footstep. This algorithm is applied for each geophone individually, and then for detection it is required that X out of M geophones receive a detection. An overview of the algorithm is seen in Fig. 1.

There are a few parameters in this method that have to be tuned depending on what standing waves are present in the ground and these may vary depending on location and weather conditions. The tuning parameters are the length of the signal segments N, the cut-off frequencies of the band-pass filter, the frequency range of the periodogram to sum, the threshold T for which the energy in the summed frequencies has to surpass for detection and how many geophones need to get a detection.

D. DOA Estimation

The seismic signal measured by geophone i is given by the signal model in (1). Using the frequency analysis explored in Section II-C, a band-pass filter is applied to remove most of the noise $e_i(t)$ in the signal. Some noise may still be present after filtering, but since the noise is assumed to be small in

amplitude compared to the signal of interest it is neglected in the following calculations.

1) NLS Estimation: To estimate the DOA of the elephant footstep, delay-and-sum is used on the measurements of $y_i(t)$ [20]. This method is based on the geometry of the array and calculates the DOA by measuring the power of the summed signals at each possible arrival angle. The maximum of the power corresponds to the estimated angle of arrival

$$y_{DS}(t,\phi) = \frac{1}{M}\sum_{i=1}^{M} y_i(t-\tau_i(\phi)) \tag{2a}$$

$$V_N(\phi) = \int_{t\in W} \left|y_{DS}(t,\phi)\right|^2 dt \tag{2b}$$

$$\hat{\phi} = \arg\max_{\phi} V_N(\phi), \tag{2c}$$

where W denotes a sliding time window covering the detected footstep from all geophones. The computations are straightforward, and the optimization is performed in discrete time on a one-dimensional grid.

2) Variance Estimation and DOA refinement: To compute the variance and refine the DOA estimate, a second degree polynomial is fit locally around the maximum

$$V_N(\phi) \approx a + b\left(\phi-\hat{\phi}\right) + c\left(\phi-\hat{\phi}\right)^2, \tag{3}$$

where the parameters a, b and c are estimated using the *least squares* (LS) method. The interval for which ϕ to include around the maximum $\hat{\phi}$ is crucial to get a good estimate of the variance. Once this polynomial is estimated, it can be shown that a refined estimate of the angle $\hat{\hat{\phi}}$ and its variance can be computed as

$$\hat{\hat{\phi}} = \hat{\phi} - \frac{b}{2c} \tag{4a}$$

$$\mathrm{Var}(\hat{\hat{\phi}}) = \frac{\frac{b^2}{4c} - a}{Nc}, \tag{4b}$$

where N is the number of samples in the sliding window W.

3) Tracking: To track the movement of the elephant a constant position *Kalman filter* (KF) is used with the DOA angle as the state, $x_k = \phi_k$,

$$x_{k+1} = x_k + w_k, \qquad w_k \sim \mathcal{N}(0, Q_k) \tag{5a}$$

$$y_k = x_k + v_k, \qquad v_k \sim \mathcal{N}(0, R_k), \tag{5b}$$

where w_k is the process noise, y_k is the DOA estimate from (4a) and v_k is the noise of the DOA estimate [21]. A constant position model is used since the elephant moves slowly, and when no step is detected the elephant is most likely standing still. The variance of v_k is R_k, which is estimated using (4b), and the variance of the process noise Q_k is a tuning parameter. Additionally, gating is used to remove false or unlikely DOA estimates

$$(y_k - \hat{y}_{k|k-1})^T S_k^{-1} (y_k - \hat{y}_{k|k-1}) < \gamma_G, \tag{6}$$

where γ_G is the gate threshold and S_k is the innovation covariance from the KF. The gate threshold is related to the probability to accept correct measurements $P_G = \int_0^{\gamma_G} \chi^2(\gamma; n_y)\, d\gamma$ where n_y is the degrees of freedom (here $n_y = 1$) [22].

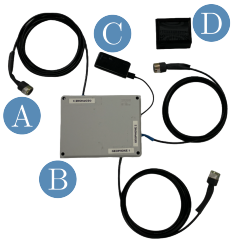

(a) Hardware overview of the complete system with the following items. **A** — Three geophones. **B** — Rain and dust resistant box containing a microcontroller, ADC and the circuitry for the geophones. **C** — Powerbank that supplies electricity to the microcontroller. **D** — Portable Raspberry Pi with a touchscreen and battery.

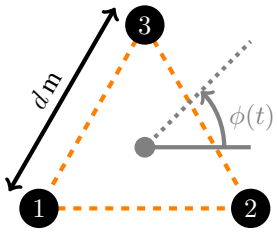

(b) The setup of the geophone network. The distance between the geophones is d meters and the DOA angle is denoted $\phi(t)$.

Fig. 2: The hardware components used and the setup of the geophone network.

III. Experiment Design

In this section the hardware design is presented as well as the experimental setup.

A. Hardware

To test the algorithm, a sensor prototype has been developed consisting of three geophones, SM-24 Geophone Element, with a bandwidth of 10 to 240 Hz. The data from the analog geophones pass an *analog to digital converter* (ADC), ADS1256, before being processed by a microcontroller board, Adafruit HUZZAH32 (ESP32-based, dual core Tensilica LX6 microcontroller). The microcontroller is powered by a powerbank, and a handheld computer (Raspberry Pi 3 Model B) with a touchscreen is used to control the device. All components are illustrated in Fig. 2a.

The geophones were positioned such that they formed the vertices in an equilateral triangle with a side length of 4 meters, as depicted in Fig. 2b. This is typically known as a *uniform circular array* (UCA) and results in the discrete geometric delays

$$\tau_1(\phi) = -\frac{f_s d}{\sqrt{3}v}\cos(\phi + 150°) \tag{7a}$$

$$\tau_2(\phi) = -\frac{f_s d}{\sqrt{3}v}\cos(\phi + 30°) \tag{7b}$$

$$\tau_3(\phi) = -\frac{f_s d}{\sqrt{3}v}\cos(\phi - 90°), \tag{7c}$$

with respect to the center of the array. Where f_s is the sampling frequency, d is the distance between the geophones and v is the propagation speed of the elephant footstep.

B. Sampling

The geophone is an electromagnet that produces a voltage when moved. To use this voltage in a meaningful way it has to be converted to a digital signal by an ADC. In theory, the ADC used has a sampling frequency of 2.5 Hz to 30 kHz, allowing for trade off between resolution and sampling speed. However,

Fig. 3: The setup of the geophone network at Kolmården. The DOA angle is denoted $\phi(t)$. The elephant walks in front of the geophones network at a distance of 15–40 m.

since the upper bandwidth of the geophones is 240 Hz, a sampling frequency above 480 Hz does not make sense.

Rayleigh waves rarely exceed 200 Hz and the waves produced by the footsteps of elephants rarely exceed 30 Hz. To avoid aliasing, the sampling frequency has to be 400 Hz or higher. Due to hardware limitations, the actual sampling frequency ended up at 474 Hz, which is sufficient for Rayleigh waves and almost entirely covers the bandwidth of the geophones.

C. Experiments

Data were collected at Kolmården Wildlife Park using the developed prototype. First, the wave propagation speed was measured by dropping a large boulder at $\phi = 0°$ for one pair of geophones. Using cross-correlation to retrieve the time delays, the wave propagation speed v was computed to be $v = 165$ m/s.

Thereafter, a male Asian elephant walked from one side of the enclosure to the other, corresponding to an angle ϕ of 30 to 150 degrees. The elephant kept a distance of approximately 15 to 40 meters from the array, as seen in Fig. 3.

IV. Results

In this section, the results of the signal analysis of the elephant footstep and ambient noise are presented to gain relevant information for the detection algorithm. This leads to the presentation of the detection, DOA estimate, and tracking results.

A. Elephant footstep

The impulse of an elephant's footstep typically look like Fig. 4a. It lasts for about 350 ms, which is a bit longer than stated in [10], as they claimed an elephant footstep to last for around 103–250 ms. By studying how the elephant walked, it was noticed that the elephant put his forefoot down around 100 ms after his hind foot. Thus, the signals originating from both the fore and hind foot have been captured within the 350 ms signal duration.

During the experiments, it was found that the frequency content of elephant footsteps depends on the composition of the ground. Early tests in the spring, with the ground still frozen, showed a higher frequency content of the signal

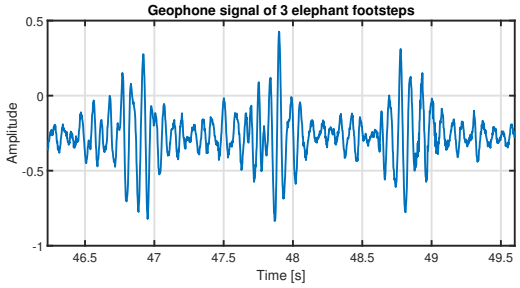

(a) Geophone signals in the time domain, where three elephant footsteps are present.

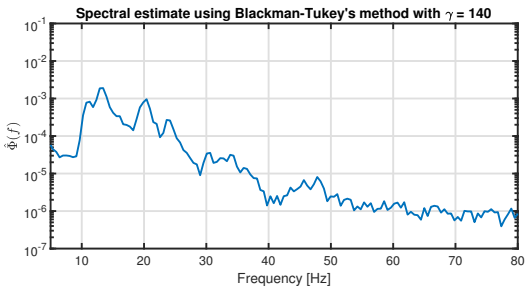

(b) A spectral estimate of the signal in Fig. 4a using Blackman-Tukey's method with γ = 140.

Fig. 4: Properties of elephant footsteps in the time and frequency domain when the elephant was walking on dry sand.

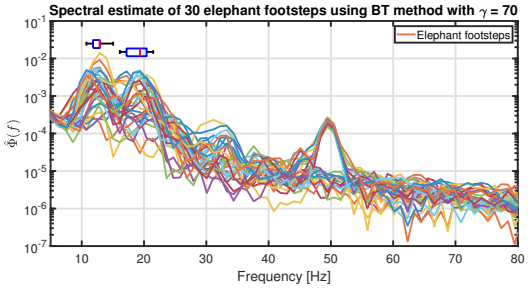

Fig. 5: Spectral estimate of 30 elephant footsteps using Blackman-Tukey's method with γ = 70 plotted in solid lines with different colors. There are two main peaks of the elephant footstep where a box plot has been added to indicate the location of the peaks.

compared to the vast majority of the experiments carried out later in the spring on dry sand. The experiments on the dry sand resulted in a main energy content around 8–23 Hz for the elephant footsteps, as seen in Fig. 4b.

By looking at 30 different footsteps, it is observed in Fig. 5 that the amplitude of the footstep varies, but the overall frequency response look similar, with one peak at around 12 Hz and a second peak around 19 Hz. The most prominent peak varies between footsteps, but the majority of the time the peak around 12 Hz has the highest amplitude. By looking at the box plot, it is seen that the first peak varies between 11–15 Hz with a median of 13 Hz, while the second peak varies between 16–21 Hz with a median of 19 Hz. Also, a lower peak around 50 Hz is present in half of the footstep, this is due to a disturbance that appeared halfway during the experiments.

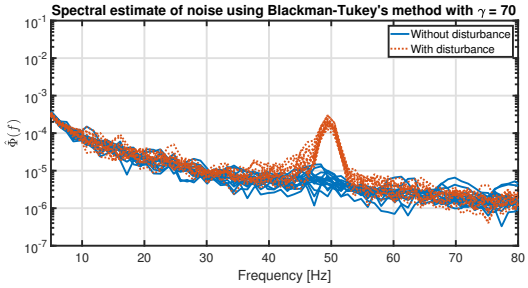

Fig. 6: Spectral estimate of 30 segments of the background noise using Blackman-Tukey's method with $\gamma = 70$. Each segment is the same length as the elephant footsteps in Fig. 5. The blue solid lines are the frequency content before the disturbance appeared, and the orange dotted lines are the frequency content with the disturbance active.

B. Background noise

An important aspect of the detection method is to analyze the background noise of the geophones. In Fig. 6 the frequency content of the background noise is shown. At first, during the data collection, the noise levels were quite low. But then, around 90 seconds in, a source of disturbance was turned on somewhere in the neighborhood, this resulted in a clear peak around 50 Hz. Compared to the frequency content of the elephant footstep in Fig. 5, there are no significant peaks around 11–19 Hz. This suggests that the main frequency content of the elephant footstep is around 8–23 Hz.

C. Detection, DOA and Tracking

As the elephant footstep was found to last for around 350 ms, the segment length should be 700 ms. With a sample frequency of 474 Hz this corresponds to a segment length of roughly $N = 350$ samples. Since the main frequency of the elephant footstep was around 8–23 Hz, the cut-off frequencies of the band-pass filter in the detection algorithm were set to 4 and 30 Hz. Then, frequencies between 8–23 Hz were summed and the threshold T in the detection algorithm was tuned. Also, the number of geophones that were needed for detection was tuned, and 2 out of 3 geophones were found to give a satisfactory result. Thereafter, the detected signal was filtered with a band-pass filter with cut-off frequencies at 8 and 23 Hz before the delay-and-sum algorithm was applied. Lastly, the interval for ϕ in the variance estimation was chosen to be $\hat{\phi} \pm 20°$. In Fig. 7 the result for different thresholds is shown for the training data.

From the training data a good trade-off between false alarms and missed detections appears to be around $T = 97\,\%$. To verify that the parameters were not over tuned to the specific data set, the tuning parameters were tested on a new validation data set. Also, tracking of the elephant was done using the Kalman filter. In order to get a satisfying performance of the tracking Q_k was set to 100 and the gating threshold to $\gamma_G = 10.83$, corresponding to a probability to accept correct measurements of 99.9 %. The results can be seen in Fig. 8.

From the figure, it is seen that the elephant is tracked with acceptable accuracy. However, since the dotted line is

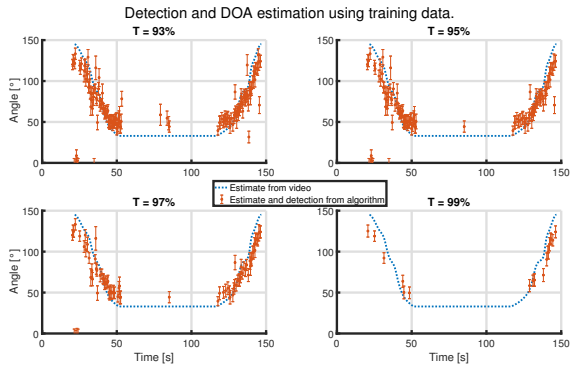

Fig. 7: The resulting detection and DOA estimation with different thresholds in the detection algorithm. The blue dotted line is the direction to the elephant estimated from a drone flying above the elephant. The measurements are presented as an orange star with a 95 % confidence interval (CI).

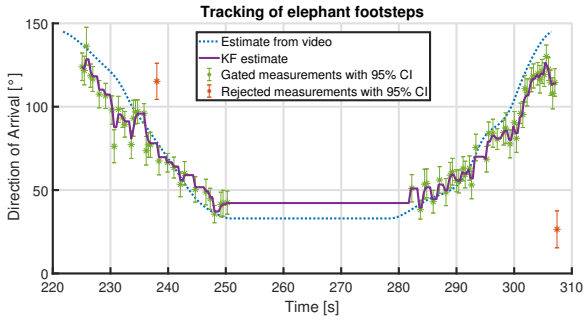

Fig. 8: The algorithm performance on the validation data. The blue dotted line is the direction to the elephant estimated from a drone flying above the elephant. The purple solid line is the KF estimate. The measurements are presented as a star with a 95 % CI, green (*) indicates gated measurements and orange (*) indicates rejected measurements from the gating.

estimated from a flying drone, it is hard to know the exact direction to the elephant, and it should not be considered as the ground truth.

V. Conclusions

In this paper, an algorithm for detection, localization and tracking of elephants has been developed with the purpose to mitigate human-wildlife conflicts. The algorithm has been tested and validated at a nearby zoo using a prototype with 3 geophones. The results show that the suggested methods work to detect and track an elephant with promising accuracy within a range of 15 to 40 meters. However, in order to further validate the tracking performance a better estimate of the ground truth is necessary.

This paper shows a proof of concept of a device capable of protecting the communities living close to national parks. The range of 40 meters would be sufficient if multiple arrays were deployed around the protected area, where the distance between the arrays is dependent on the range. In order to deploy this device in a real scenario, the algorithms must

be adapted to cope with different weather conditions on the savanna, as well as the ambient noise.

Future research includes to investigate how the method works with other individuals of elephants of different sizes and weights. It is also of interest to examine how a heard of elephants would affect the detection and DOA estimate, and to apply a multi target tracking framework to track multiple elephants. Further, since ground vehicles generate noise around the frequencies of an elephant footstep, it would be interesting to study the effect of nearby vehicles. Also, the disturbance from other mammals walking in the area would be interesting to investigate, e.g., humans, giraffes, rhinos, etc. Another idea is to add an additional network of geophones in a vicinity, to make it possible to track the position of the elephant and not only the DOA. Finally, since this method works well within 40 meters, it would be intriguing to explore the range limit of the method.

REFERENCES

[1] A. Newsfeed, "Kenya's human-elephant conflict," 2020, accessed: 2022-11-10. [Online]. Available: https://www.aljazeera.com/program/newsfeed/2020/11/26/kenyas-human-elephant-conflict

[2] S. Ganesh, "Human-elephant conflict kills 1,713 people, 373 pachyderms in 3 years," 2019, accessed: 2022-11-10. [Online]. Available: https://www.thehindu.com/news/national/human-elephant-conflict-kills-1713-people-373-pachyderms-in-3-years/article26225515.ece

[3] R. Hoare, "Lessons from 15 years of human-elephant conflict mitigation: Management considerations involving biological, physical and governance issues in Africa," *Pachyderm*, vol. 51, pp. 60–74, 2012.

[4] P. Anghelescu, G. V. Iana, and I. Tramandan, "Human footstep detection using seismic sensors," in *2015 7th International Conference on Electronics, Computers and Artificial Intelligence (ECAI)*. Bucharest, Romania: IEEE, 2015, pp. AE–1.

[5] G. Koç and K. Yegin, "Footstep and vehicle detection using seismic sensors in wireless sensor network: Field tests," *International Journal of Distributed Sensor Networks*, vol. 9, no. 10, p. 120386, 2013.

[6] R. Ghosh, A. Akula, S. Kumar, and H. Sardana, "Time–frequency analysis based robust vehicle detection using seismic sensor," *Journal of Sound and Vibration*, vol. 346, pp. 424–434, 2015.

[7] J. Altmann, S. Linev, and A. Weiß, "Acoustic–seismic detection and classification of military vehicles—developing tools for disarmament and peace-keeping," *Applied Acoustics*, vol. 63, no. 10, pp. 1085–1107, 2002.

[8] E. Suriñach, I. Vilajosana, G. Khazaradze, B. Biescas, G. Furdada, and J. M. Vilaplana, "Seismic detection and characterization of landslides and other mass movements," *Natural Hazards and Earth System Sciences*, vol. 5, no. 6, pp. 791–798, 2005.

[9] C. E. O'Connell-Rodwell, "Keeping an "ear" to the ground: seismic communication in elephants," *Physiology*, vol. 22, no. 4, pp. 287–294, 2007.

[10] C. E. O'Connell-Rodwell, B. T. Arnason, and L. A. Hart, "Seismic properties of Asian elephant (Elephas maximus) vocalizations and locomotion," *The Journal of the Acoustical Society of America*, vol. 108, no. 6, pp. 3066–3072, 2000.

[11] M. Reinwald, B. Moseley, A. Szenicer, T. Nissen-Meyer, S. Oduor, F. Vollrath, A. Markham, and B. Mortimer, "Seismic localization of elephant rumbles as a monitoring approach," *Journal of The Royal Society Interface*, vol. 18, 2021.

[12] J. H. Poole, "Behavioral contexts of elephant acoustic communication," *The Amboseli elephants: a long-term perspective on a long-lived mammal. Chicago: The University of Chicago*, pp. 125–161, 2011.

[13] J. D. Wood, C. E. O'Connell-Rodwell, and S. L. Klemperer, "Using seismic sensors to detect elephants and other large mammals: a potential census technique," *Journal of Applied Ecology*, vol. 42, no. 3, pp. 587–594, 2005.

[14] A. Szenicer, M. Reinwald, B. Moseley, T. Nissen-Meyer, Z. Mutinda Muteti, S. Oduor, A. McDermott-Roberts, A. G. Baydin, and B. Mortimer, "Seismic savanna: machine learning for classifying wildlife and behaviours using ground-based vibration field recordings," *Remote Sensing in Ecology and Conservation*, vol. 8, no. 2, pp. 236–250, 2022.

[15] S. Alyamkin and E. Nezhevenko, "Comparative analysis of the efficiency of the Kalman filter and particle filter in solving the problem of object tracking in a seismic security system," *Optoelectronics, Instrumentation and Data Processing*, vol. 50, pp. 54–60, 2014.

[16] C. J. Ammon, A. A. Velasco, T. Lay, and T. C. Wallace, "Chapter 1 - An overview of global seismology," in *Foundations of Modern Global Seismology (Second Edition)*, C. J. Ammon, A. A. Velasco, T. Lay, and T. C. Wallace, Eds. Academic Press, 2021, pp. 3–37.

[17] S. C. Webb, "Chapter 19 - Seismic Noise on Land and on the Sea Floor," in *International Handbook of Earthquake and Engineering Seismology, Part A*, ser. International Geophysics, W. H. Lee, H. Kanamori, P. C. Jennings, and C. Kisslinger, Eds. Academic Press, 2002, vol. 81, pp. 305–318.

[18] M. E. Kappus and F. L. Vernon, "The acoustic signature of thunder from seismic records," *The Journal of the Acoustical Society of America*, vol. 88, no. S1, pp. S191–S191, 1990.

[19] N. Riahi and P. Gerstoft, "The seismic traffic footprint: Tracking trains, aircraft, and cars seismically," *Geophysical Research Letters*, vol. 42, no. 8, pp. 2674–2681, 2015.

[20] H. L. V. Trees, *Optimum Array Processing: Part IV of Detection, Estimation, and Modulation Theory*. John Wiley & Sons, Ltd, 2002.

[21] R. E. Kalman, "A New Approach to Linear Filtering and Prediction Problems," *Journal of Basic Engineering*, vol. 82, no. 1, pp. 35–45, 1960.

[22] S. K. Singh, M. Premalatha, and G. Nair, "Ellipsoidal gating for an airborne track while scan radar," in *Proceedings International Radar Conference*. Alexandria, VA, USA: IEEE, 1995, pp. 334–339.